**An Approach to Producing Space-Time Covariance Functions on Spheres**
Mikyoung Jun; Michael L Stein
*Technometrics;* Nov 2007; 49, 4; ABI/INFORM Global
pg. 468

# An Approach to Producing Space–Time Covariance Functions on Spheres

**Mikyoung JUN**
Department of Statistics
Texas A&M University
College Station, TX 77843
(*mjun@stat.tamu.edu*)

**Michael L. STEIN**
Department of Statistics
University of Chicago
Chicago, IL 60637
(*stein@galton.uchicago.edu*)

For space–time processes on global or large scales, it is critical to use models that respect the Earth's spherical shape. The covariance functions of such processes should be not only positive definite on sphere × time, but also capable of capturing the dynamics of the processes well. We develop space–time covariance functions on sphere × time that are flexible in producing space–time interactions, especially space–time asymmetries. Our idea is to consider a sum of independent processes in which each process is obtained by applying a first-order differential operator to a fully symmetric process on sphere × time. The resulting covariance functions can produce various types of space–time interactions and give different covariance structures along different latitudes. Our approach yields explicit expressions for the covariance functions, which has great advantages in computation. Moreover, it applies equally well to generating asymmetric space–time covariance functions on flat or other spatial domains. We study various characteristics of our new covariance functions, focusing on their space–time interactions. We apply our model to a dataset of total column ozone levels in the Northern hemisphere.

KEY WORDS: Matérn model; Separable covariance function; Space–time asymmetry; Total column ozone.

## 1. INTRODUCTION

Geophysical and environmental processes generally vary in both space and time, and their spatial domain is the spherical Earth. Much environmental data, such as satellite data, cover a large portion of the Earth. Series expansions of spherical harmonics as a model for stochastic processes on the sphere have been considered for some time in the statistical and geodetic sciences (Yaglom 1961; Jones 1963; Grafarend 1976; McLeod 1986). Oh and Li (2004) used spherical wavelets for modeling surface air temperature observations on the whole globe.

For producing explicit covariance functions for isotropic processes on a sphere, many authors (Yaglom 1987; Weber and Talkner 1993; Gaspari and Cohn 1999; Gneiting 1999) have focused on the simple idea of restricting covariance functions in $\mathbb{R}^d$ to $\mathcal{S}_r^{d-1}$, a sphere with radius $r$. We call a process on the sphere isotropic if its covariance depends only on the spherical distance between two points and its mean is constant (Jones 1963). All of these works deal with the spatial domain only, however. For the space–time domain, some space–time covariance functions for processes on flat surfaces have been developed (Jones and Zhang 1997; Cressie and Huang 1999; Gneiting 2002; de Iaco, Myers, and Posa 2002; Ma 2003; Stein 2005a). Nevertheless, there has been little research on developing space–time covariance functions for a spherical domain; exceptions include the work of McLeod (1996) and Stein (2005b), which discussed some simple methods for generating such models with none or rather limited space–time interactions.

For data sets with global coverage, treating the spatial domain as flat clearly distorts reality, because there is no way to map a sphere to a plane continuously and invertibily. Considering the increasing commonness of data sets with global coverage, it is imperative to develop covariance functions on spherical surfaces. In particular, for many global processes, covariances are likely to change substantially with latitude in such a way that models based on a flat spatial domain are not intended to capture. Even when the spatial domain is not quite global, space–time covariance functions on spherical surfaces can still be important to capture dependencies on latitude and effects due to flows circling the Earth.

Some authors have noticed *space–time asymmetry* in wind and air pollution data (Gneiting 2002; Jun and Stein 2004; Stein 2005a,b). As done by Gneiting (2002), we call a space–time process $Z$ *fully symmetric* if $\mathrm{cov}\{Z(\mathbf{s}_1, t_1), Z(\mathbf{s}_2, t_2)\} = \mathrm{cov}\{Z(\mathbf{s}_1, t_2), Z(\mathbf{s}_2, t_1)\}$ for all locations $\mathbf{s}_1$ and $\mathbf{s}_2$ and time points $t_1$ and $t_2$. Space–time asymmetry means that these two covariances are not always the same. Space–time separable models, commonly used for their simplicity (Posa 1993; Haas 1995; Mitchell and Gumpertz 2003), are necessarily fully symmetric.

Stein (2005b) described two ways of constructing space–time covariance functions on sphere × time that produce space–time asymmetry. Consider the Earth's surface as our spatial domain and let $L$ denote latitude, $l$ denote longitude, $t$ denote time, $r$ denote the Earth's radius, and $\mathcal{S}_r^2$ denote Earth's surface. For a space–time process $Z(L, l, t)$ on $\mathcal{S}_r^2 \times \mathbb{R}$, Stein (2005b) described what we call *rotation models* as a simple way of generating asymmetry. The chordal distance between the two points on $\mathcal{S}_r^2$, $(L_1, l_1)$ and $(L_2, l_2)$, is given by

$$\mathrm{ch}(L_1, L_2, l_1 - l_2) = 2r\left\{\sin^2\left(\frac{L_1 - L_2}{2}\right) + \cos L_1 \cos L_2 \sin^2\left(\frac{l_1 - l_2}{2}\right)\right\}^{1/2}.$$

© 2007 American Statistical Association and
the American Society for Quality
TECHNOMETRICS, NOVEMBER 2007, VOL. 49, NO. 4
DOI 10.1198/004017007000000155



Reproduced with permission of the copyright owner. Further reproduction prohibited without permission.

The covariance function of a rotation model is of the form

$$\operatorname{cov}\big(Z(L_1, l_1, t_1), Z(L_2, l_2, t_2)\big) = K\big(\operatorname{ch}\big(L_1, L_2, l_1 - l_2 - \epsilon(t_1 - t_2)\big), t_1 - t_2\big)$$

for $\widetilde{K}(\mathbf{s}, t) = K(|\mathbf{s}|, t)$, with $\widetilde{K}$ a valid covariance function on $\mathbb{R}^3 \times \mathbb{R}$, where $|\cdot|$ denotes the Euclidean norm. Such rotation models are valid for processes on $\mathcal{S}_r^2 \times \mathbb{R}$ and can produce space–time asymmetry for an east–west flow. But this model implies that the speed of flow on the Earth slows as one gets closer to the poles. This method may not provide an adequate representation of space–time asymmetries over a wide range of latitudes. A partially nonparametric method of Stein (2005b) for producing space–time covariance functions on $\mathcal{S}_r^2 \times \mathbb{R}$ is somewhat limited in explaining space–time interaction in the sense that it produces asymmetry in only a fixed direction over the whole domain. Moreover, this approach does not generally yield explicit expressions for the covariance function.

We propose a new way of constructing valid space–time covariance functions on sphere × time that are weakly stationary with respect to longitude and time for fixed values of latitude. Our new covariance functions have many desirable features. First, they provide a rich class of space–time interactions. They allow interactions between latitude, longitude, and time, so that many different types of asymmetries can be represented. In particular, they can give different directions of space–time asymmetries along latitudes, longitudes or time. Moreover, unlike rotation models, the speed of flow can be kept nearly constant at different latitudes or not constant, if necessary. Second, our new models naturally produce different covariance structures along different latitudes. This can be advantageous when the spatial domain includes a large range of latitudes and covariance structures are clearly different at different latitudes. For example, Fang and Stein (1998) showed that the covariance structure of total column ozone at a given latitude depends strongly on latitude. Third, our models yield explicit expressions for the covariance function. This is of considerable value when spectral methods are difficult to apply, such as when observations are sporadic in time and/or space or we are interested in prediction at many locations other than the observation sites.

The approach that we describe for producing covariance functions on sphere × time also can be used to produce asymmetric covariance functions on a flat space crossed with time and similarly yields richer classes of asymmetry than the approaches described by Stein (2005a). The focus here is on the spherical domain because the greater flexibility in space–time interactions will be more critical for processes on a global scale, for which the spherical spatial domain is necessary.

## 2. COVARIANCE FUNCTIONS ON A SPHERICAL DOMAIN

A central challenge in developing spatial covariance functions for processes on the sphere is to find explicit expressions for valid covariance functions. It is known that the covariance function of an isotropic random process on $\mathcal{S}_r^2$ is characterized by an infinite sum of Legendre polynomials with nonnegative coefficients and cosine of the great circle distance as their argument (Yaglom 1987). This infinite sum is strictly positive definite on a sphere if all of the coefficients of these polynomials are nonnegative with only a finite number of them being zero (Schreiner 1997). Only a few closed forms for such infinite sums are known, and thus in general we do not have explicit expressions for the covariance functions. Moreover, in many applications, these known closed forms may not be rich enough to describe the covariance structure of processes. We could take a finite convex combination of these known closed forms or even a finite convex combination of Legendre polynomials (Das 2000). However, although the finite convex combination of Legendre polynomials is positive definite, it gives an analytic covariance function, which Stein (1999) criticized as being unrealistically smooth for natural processes.

As suggested by Yaglom (1987, p. 389), we can take isotropic spatial covariance functions in $\mathbb{R}^3$ with chordal distance on $\mathcal{S}_r^2$ (equivalently, Euclidean distance in $\mathbb{R}^3$) to get valid covariance functions on $\mathcal{S}_r^2$. Then we get isotropic covariance functions on $\mathcal{S}_r^2$. Because there are various isotropic covariance functions available for spatial processes in $\mathbb{R}^3$, as noted by Gneiting (1999), this method can give a fairly rich class of isotropic covariance functions on spherical domains.

When we add time to our domain, we can still apply the idea of Yaglom (1987) to get valid space–time covariance functions on sphere × time. Let us denote the points on the spherical domain, $\mathbf{s}_i = (L_i, l_i) \in \mathcal{S}_r^2$, and the points in the temporal domain, $t_i \in \mathbb{R}$ for $i = 1, 2$. Denote $(L_i, l_i, t_i) \in [-\frac{1}{2}\pi, \frac{1}{2}\pi] \times \mathbb{T} \times \mathbb{R}$, $i = 1, 2$, where $\mathbb{T}$ is the real line mod $2\pi$. Because we can consider the $\mathbf{s}_i$'s as points in $\mathbb{R}^3$, let $\widetilde{\mathbf{s}}_i \in \mathbb{R}^3$ be $\mathbf{s}_i$ in the Euclidean coordinate system and let $\boldsymbol{\tau}_i = (\widetilde{\mathbf{s}}_i, t_i) \in \mathbb{R}^4$, $i = 1, 2$. Define a distance in $\mathbb{R}^4$, $d_4(\boldsymbol{\tau}_1, \boldsymbol{\tau}_2) = h_0(|\widetilde{\mathbf{s}}_1 - \widetilde{\mathbf{s}}_2|, |t_1 - t_2|)$ for a suitable function $h_0$. Let $\psi : [0, \infty) \to \mathbb{R}$ be a continuous function so that $\psi(d_4(\cdot, \cdot))$ is an autocovariance function on $\mathbb{R}^4$. Now we restrict $\psi$ to the domain of sphere × time by the approach of Yaglom (1987) in the following way. Noting that $|\widetilde{\mathbf{s}}_1 - \widetilde{\mathbf{s}}_2| = \operatorname{ch}(L_1, L_2, l_1 - l_2)$, consider $f : [0, \infty) \to \mathbb{R}$ continuous with $f(h_0(\operatorname{ch}(L_1, L_2, l_1 - l_2), |t_1 - t_2|)) = \psi(d_4(\boldsymbol{\tau}_1, \boldsymbol{\tau}_2))$. Then $f(h_0(\operatorname{ch}(\cdot, \cdot, \cdot), |\cdot|))$ is positive definite on $[-\frac{1}{2}\pi, \frac{1}{2}\pi]^2 \times \mathbb{T} \times \mathbb{R}$ and thus gives a valid covariance function for processes on $\mathcal{S}_r^2 \times \mathbb{R}$. Processes with such covariance functions are invariant with respect to all rotations on the sphere and translations in time. These covariance functions are fully symmetric in space–time. As a special case, for $\beta_1, \beta_2 > 0$, define

$$\begin{aligned} &h(L_1, L_2, l_1 - l_2, t_1 - t_2) \\ &\quad = h_0^2\big(\operatorname{ch}(L_1, L_2, l_1 - l_2), |t_1 - t_2|\big) \\ &\quad = \beta_1^2 \operatorname{ch}^2(L_1, L_2, l_1 - l_2) + \beta_2^2 (t_1 - t_2)^2 \end{aligned} \tag{1}$$

and $d_4(\boldsymbol{\tau}_1, \boldsymbol{\tau}_2) = \{\beta_1^2 |\widetilde{\mathbf{s}}_1 - \widetilde{\mathbf{s}}_2|^2 + \beta_2^2 (t_1 - t_2)^2\}^{1/2}$. Then, $f(h^{1/2}(\cdot, \cdot, \cdot, \cdot))$ is a valid covariance function for processes on $\mathcal{S}_r^2 \times \mathbb{R}$.

The fact that $h$ is defined in terms of chordal distance is not critical here. We work with chordal distance only because through chordal distance, we can restrict positive definite covariance functions on $\mathbb{R}^3$ to $\mathcal{S}_r^2$. Nevertheless, due to the one-to-one relationship between chordal distance and great circle distance, we could just as well express $h$ as a function of great circle distance and $f$ would then have great circle distance as its argument rather than chordal distance.



Reproduced with permission of the copyright owner. Further reproduction prohibited without permission.

## 3. ASYMMETRIC COVARIANCE FUNCTIONS ON SPHERE × TIME

The main goal in this article is to produce closed forms for asymmetric covariance functions on sphere × time. Our idea is to apply differential operators to fully symmetric processes and then consider the covariance functions of such processes. Let $\mathbb{S}$ denote such a spatial domain with $d$ coordinates and $\mathbf{s} = (s_1, \ldots, s_d) \in \mathbb{S}$. Let $\mathcal{D}(\mathbb{S})$ be the class of (not necessarily stationary) real space–time random fields on $\mathbb{S} \times \mathbb{R}$ with finite second moments whose directional derivatives along each axis exist. For $Z(\mathbf{s}, t) \in \mathcal{D}(\mathbb{S})$ and nonrandom, continuous functions $\alpha_i(\mathbf{s}, t)$'s, $i = 1, \ldots, d+1$, and $t \in \mathbb{R}$, define

$$X[Z; \alpha_1, \ldots, \alpha_{d+1}](\mathbf{s}, t) = \left\{\alpha_1(\mathbf{s}, t)\frac{\partial}{\partial s_1} + \cdots + \alpha_d(\mathbf{s}, t)\frac{\partial}{\partial s_d} + \alpha_{d+1}(\mathbf{s}, t)\frac{\partial}{\partial t}\right\}Z(\mathbf{s}, t). \quad (2)$$

Let $K$ be the covariance function of $Z$. Denote the covariance function of $X[Z; \alpha_1, \ldots, \alpha_{d+1}]$ by

$$K_X[K; \alpha_1, \ldots, \alpha_{d+1}](\mathbf{s}_1, \mathbf{s}_2, t_1, t_2) = \operatorname{cov}\big(X[Z; \alpha_1, \ldots, \alpha_{d+1}](\mathbf{s}_1, t_1), X[Z; \alpha_1, \ldots, \alpha_{d+1}](\mathbf{s}_2, t_2)\big).$$

We can generalize this idea of applying differential operators to space–time processes on any spatial domain as long as a coordinate system and differentiation can be defined on the domain (i.e., differentiable manifolds). As an example, we show how to use this approach to reproduce a class of asymmetric covariance functions described by Stein (2005a) for a flat spatial domain. As done by Stein (2005a), let $K$, the covariance function of $Z \in \mathcal{D}(\mathbb{R}^2)$, be given by $K(\mathbf{s}, t) = \int_{\mathbb{R}^2 \times \mathbb{R}} \exp(i\mathbf{w}^T\mathbf{s} + ivt)g(\mathbf{w}, v)\,\mathbf{dw}\,dv$, where $g$ is the corresponding spectral density. Then $Z$ is stationary with respect to space and time. Suppose that $K$ is spatially and temporally isotropic in the sense that $g(\mathbf{w}, v) = g_1(|\mathbf{w}|, |v|)$, so that $K$ is fully symmetric, and suppose further that $(1 + |\mathbf{w}|^2 + v^2)g_1(|\mathbf{w}|, |v|) \geq 0$ is integrable over $\mathbb{R}^2 \times \mathbb{R}$. For $\mathbf{z} = (z_1, z_2)^T \in \mathbb{R}^2$ a unit vector; scalars $a$, $c_1$, and $c_2$ nonnegative; and $b^2 \leq 4c_1c_2$, consider the spectral density $g_2(\mathbf{w}, v) = (a + b(\mathbf{w}^T\mathbf{z})v + c_1|\mathbf{w}|^2 + c_2v^2)g_1(|\mathbf{w}|, |v|)$. The vector $\mathbf{z}$ is the direction of the asymmetry. Then, as noted by Stein (2005a), the covariance function $K_2$ given by the Fourier transform of $g_2$ can be written in terms of derivatives of $K$. There does not appear to be a simple way to extend this approach directly to obtain explicit expressions for covariance functions on sphere × time, which led us to the alternative of differentiating space–time *processes* on the sphere. To see that this approach can yield $K_2$, let $Z_0, \ldots, Z_5$ be iid copies of $Z$, each with spectral density $g$. For $\delta_1$ and $\delta_2$ constants with $|\delta_1|, |\delta_2| < \sqrt{c_1}$, consider the process

$$a^{1/2}Z_0 + X[Z_1; \delta_1, 0, 0] + X[Z_2; 0, \delta_2, 0] + X[Z_3; 0, 0, c_2] + X\left[Z_4; \sqrt{c_1 - \delta_1^2}, 0, \frac{bz_1}{2\sqrt{c_1 - \delta_1^2}}\right] + X\left[Z_5; 0, \sqrt{c_1 - \delta_2^2}, \frac{bz_2}{2\sqrt{c_1 - \delta_2^2}}\right]. \quad (3)$$

We can then show that the covariance function of (3), $aK + K_X[K; \delta_1, 0, 0] + K_X[K; 0, \delta_2, 0] + K_X[K; 0, 0, \delta_3] + K_X[K; \sqrt{c_1 - \delta_1^2}, 0, bz_1/(2\sqrt{c_1 - \delta_1^2})] + K_X[K; 0, \sqrt{c_1 - \delta_2^2}, bz_2/(2 \times \sqrt{c_1 - \delta_2^2})]$, is equal to $K_2$, as desired. This is due to the fact that for any constants $\eta_1$, $\eta_2$, and $\eta_3$, $K_X[K; \eta_1, \eta_2, \eta_3](x_1, x_2, x_3) = -\sum_{i,j=1}^{3} \eta_i\eta_j \frac{\partial^2}{\partial x_i \partial x_j}K(x_1, x_2, x_3)$, $\mathbf{x} = (x_1, x_2, x_3) \in \mathbb{R}^3$.

Now we return to the domain of interest here, $\mathcal{S}_r^2 \times \mathbb{R}$. Let $\mathcal{K}$ be the class of real-valued functions on $[-\frac{1}{2}\pi, \frac{1}{2}\pi]^2 \times \mathbb{T} \times \mathbb{R}$ satisfying the following two conditions: for $K_0 \in \mathcal{K}$,

$$K_0(L_1, L_2, l, t) = K_0(L_2, L_1, -l, -t) \quad \text{for } L_1, L_2 \in \left[-\frac{1}{2}\pi, \frac{1}{2}\pi\right], l \in \mathbb{T} \text{ and } t \in \mathbb{R}$$

and

$$\sum_{j,k=1}^{n} \rho_j\rho_k K_0(L_j, L_k, l_j - l_k, t_j - t_k) \geq 0$$

for all real $\rho_1, \ldots, \rho_n, t_1, \ldots, t_n$; all $l_1, \ldots, l_n \in \mathbb{T}$; all $L_1, \ldots, L_n \in \left[-\frac{1}{2}\pi, \frac{1}{2}\pi\right]$; and all $n \in \mathbb{N}$.

If a process $Z \in \mathcal{D}(\mathcal{S}_r^2)$ is stationary with respect to longitude and time, then its covariance function $K$, $\operatorname{cov}(Z(L_1, l_1, t_1), Z(L_2, l_2, t_2)) = K(L_1, L_2, l_1 - l_2, t_1 - t_2)$, is in $\mathcal{K}$. Suppose that $K(L_1, L_2, l, t) = f(h^{1/2}(L_1, L_2, l, t))$, where $f$ and $h$ are as defined in Section 2. Defining $K$ in this way gives $Z$ full symmetry. For $Z$ to have directional derivatives along each axis, we need $f'(0) = 0$ and $f$ to have a continuous second derivative. Now for continuous functions $a$, $b$, and $c$ depending only on latitude, we can consider a process $X[Z; a, b, c]$ defined by (2). This process has a covariance function in $\mathcal{K}$ and is generally space–time asymmetric. Note that the covariance function of $X$ is what Jones (1963) called axially symmetric.

Allowing the functions $a$, $b$, and $c$ to depend on latitude rather than keeping them constant gives flexibility in asymmetries and possibly different covariance structures along different latitudes. We could allow $a$, $b$, and $c$ to depend on longitude or time, but then the resulting process generally will not be stationary with respect to longitude and time. Because the covariance function depends only on $L_1$, $L_2$, $l_1 - l_2$, and $t_1 - t_2$, we write it as

$$K_X[K; a, b, c](L_1, L_2, l_1 - l_2, t_1 - t_2) = \operatorname{cov}\big(X[Z; a, b, c](L_1, l_1, t_1), X[Z; a, b, c](L_2, l_2, t_2)\big).$$

Let $K^{(i_1, i_2, i_3, i_4)}$ denote

$$K^{(i_1, i_2, i_3, i_4)}(L_1, L_2, l, t) = \frac{\partial^{i_1}\,\partial^{i_2}\,\partial^{i_3}\,\partial^{i_4}}{\partial L_1\,\partial L_2\,\partial l\,\partial t}K(L_1, L_2, l, t)$$

for $i_j = 0, 1, 2$ ($j = 1, 2, 3, 4$). We have

$$\begin{aligned} K_X[K; a, b, c](L_1, L_2, l, t) &= a(L_1)a(L_2)K^{(1,1,0,0)} - b(L_1)b(L_2)K^{(0,0,2,0)} \\ &\quad - c(L_1)c(L_2)K^{(0,0,0,2)} \\ &\quad - a(L_1)b(L_2)K^{(1,0,1,0)} + a(L_2)b(L_1)K^{(0,1,1,0)} \quad (4) \\ &\quad - a(L_1)c(L_2)K^{(1,0,0,1)} + a(L_2)c(L_1)K^{(0,1,0,1)} \quad (5) \\ &\quad - \{b(L_1)c(L_2) + b(L_2)c(L_1)\}K^{(0,0,1,1)}, \quad (6) \end{aligned}$$



Reproduced with permission of the copyright owner. Further reproduction prohibited without permission.

and $K_X[K; a, b, c]$ is in $\mathcal{K}$. The terms in (4) are from the cross-product of $\frac{\partial}{\partial L}$ and $\frac{\partial}{\partial l}$ and thus give the *interactions* between latitude and longitude. Similarly, (5) gives the interactions between latitude and time, and (6) gives the interactions between longitude and time. In principle, we can take any $K$ in $\mathcal{K}$ for which $Z$ has directional derivatives along each axis. In practice, it is helpful to take $K$ to have an explicit expression that can be easily computed.

The covariance function of $X[Z; a, b, c]$ may not be appropriate for explaining some types of space–time interactions. For example, with just a single $X$ and assuming that $a$, $b$, and $c$ are constant functions, we cannot get a model with interactions between longitude and time and between latitude and time without also getting an interaction between latitude and longitude. To exclude the interactions between latitude and longitude, we need to have $ab = 0$, and this results in no interaction between latitude and time or between longitude and time. Therefore, we need to extend the approach further, so that we can produce any kind of interaction while excluding other interactions that we do not want. We also may include a fully symmetric term in the generalized process, so that the model can be reduced to a fully symmetric model if necessary. Let $Z_0, Z_1, \ldots, Z_N$ be iid copies of $Z$, each with covariance function $K$. For fixed integer $N$ and functions $a_k$, $b_k$, and $c_k$ depending only on latitude, $k = 1, \ldots, N$, consider the process

$$Y(L, l, t) = \sum_{k=1}^{N} X[Z_k; a_k, b_k, c_k](L, l, t) + d_0 Z_0(L, l, t).$$

The process $Y$ is stationary with respect to longitude and time, and its covariance function, $K_Y$, is given by

$$K_Y(L_1, L_2, l, t) = \sum_{k=1}^{N} K_X[K; a_k, b_k, c_k](L_1, L_2, l, t) + d_0^2 K(L_1, L_2, l, t). \quad (7)$$

It is not necessary that the $Z_k$'s have the same distribution, although this simplification is helpful for estimation. In practice, one may particularly want to allow $Z_0$ to follow a different law than the other $Z_k$'s.

We can get explicit expressions for the partial derivatives of $K$ in (4), (5), and (6) using derivatives of the function $f$ in the following way. Define $h_p = \frac{\partial h}{\partial x_p}$ and $h_{pq} = \frac{\partial^2 h}{\partial x_p \partial x_q}$, where $x_1 = L_1$, $x_2 = L_2$, $x_3 = l_1 - l_2$, and $x_4 = t_1 - t_2$. Then we have

$$\begin{aligned} K^{(i_1,i_2,i_3,i_4)} &= \frac{f''(\sqrt{h})}{4h} h_p h_q + \frac{f'(\sqrt{h})}{2}\left(-\frac{h_p h_q}{2h\sqrt{h}} + \frac{h_{pq}}{\sqrt{h}}\right) \\ &= \frac{h_p h_q}{4h}\left\{f''(\sqrt{h}) - \frac{f'(\sqrt{h})}{\sqrt{h}}\right\} + \frac{f'(\sqrt{h})}{\sqrt{h}}\frac{h_{pq}}{2}, \end{aligned} \quad (8)$$

where $(p, q) = \{j | i_j \neq 0\}$ if no $i_j = 2$ and $p = q = j$ if $i_j = 2$. We give explicit expressions for $h_p$ and $h_{pq}$ in Appendix A. Using those expressions, we can show that $h_{pq}$ is bounded and so is $h_p h^{-1/2}$ if we define it by continuity as $h \downarrow 0$. Moreover, because $f''$ exists and is continuous, we have that $f''(h^{1/2}) - f'(h^{1/2})h^{-1/2} = o(1)$ and $f'(h^{1/2})h^{-1/2} = f''(0) + o(1)$ as $h \downarrow 0$. Thus, when $h = 0$, we can define $K^{(i_1,i_2,i_3,i_4)} = f''(0)h_{pq}/2$. Note that $K_Y(L, L, 0, 0)$ is the variance of the process $Y$ at latitude $L$. Although we may want to allow it to vary with latitude in some situations, it generally should be bounded in $L$. Combining (7) and (8) and using Appendix A, we can show that as long as $a_k^2(L) + b_k^2(L)\cos^2 L$ and $c_k(L)$ are bounded for all $L$, $K_Y(L, L, 0, 0)$ is bounded as well.

## 4. EXAMPLE: MATÉRN–LIKE COVARIANCE FUNCTION

Although the expressions for $K_X$ and $K_Y$ may seem complicated, once we choose $K$, the form of $K_Y$ often reduces to a fairly simple formula and is not much more difficult to compute than $K$. Suppose that we let $f(x) = \alpha \mathcal{M}_{\nu+1}(x)$, a Matérn covariance function with $\nu > 0$. Here $\mathcal{M}_\nu(x) = x^\nu \mathcal{K}_\nu(x)$, where $\mathcal{K}_\nu$ is a modified Bessel function (Abramowitz and Stegun 1965) and $\nu$ is a parameter that represents the differentiability of the random field. The larger the $\nu$, the smoother the corresponding random field. For $f$, we need to have smoothness parameter greater than 1 ($\nu + 1 > 1$) since $f$ should have a continuous second derivative and $f'(0) = 0$, as explained in Section 3. Using $f'(x) = -\alpha x \mathcal{M}_\nu(x)$, $f''(x) = -\alpha \mathcal{M}_\nu(x) + \alpha x^2 \mathcal{M}_{\nu-1}(x)$, and $\mathcal{M}_{\nu+1}(x) = x^2 \mathcal{M}_{\nu-1}(x) + 2\nu \mathcal{M}_\nu(x)$ (Abramowitz and Stegun 1965), we have

$$K_Y(L_1, L_2, l, t) = C_1 \mathcal{M}_{\nu-1}(\sqrt{h}) + C_2 \mathcal{M}_\nu(\sqrt{h}) \quad (9)$$

for functions $C_1$ and $C_2$, expressible as sums of products of the $a_k$'s, $b_k$'s, $c_k$'s, $d_0$, $\alpha$, and the partial derivatives of $h$. Explicit expressions for $C_1$ and $C_2$ are given in Appendix A.

We study the behavior of (9) [in particular, a special case of (7) when $N = 2$] for various parameter values. As defined in (1), $\beta_1$ and $\beta_2$ are the inverses of the spatial and temporal ranges, so that larger values of $\beta_1$, say, correspond to a more slowly decaying spatial correlation. (For further discussion of range parameters, see Cressie 1993). Here we use km as the unit of distance and day as the unit of time. The contour plots in Figures 1 and 2 display the correlations between a fixed center location and the neighboring locations at certain time lags. For example, if $(L_1, l_1)$ is the center location, then the contour plots display $K_Y(L_1, L, l_1 - l, -t)/\sqrt{K(L_1, L_1, 0, 0)K(L, L, 0, 0)}$ for various $(L, l)$ values at some $t$. The great circle distance between the center location and any of the neighboring locations on $\mathcal{S}_r^2$ is proportional to the Euclidean distance in the pictures. Thus, if the purely spatial part of the covariance function is a function of just the great circle distance (or, equivalently, of the arclength distance), then the contours will be circular.

We choose various forms for $a_k$, $b_k$, and $c_k$ to study the behavior of $K_Y$, selected based in part on the fits to the ozone data in Section 6. Section 5 provides further discussion on the choices of $a_k$, $b_k$, and $c_k$. For $a_{0k}$, $b_{0k}$, and $c_{0k}$ constants, $k = 1, 2$, a natural choice for these functions turns out to be

$$a_k(L) = a_{0k}, \qquad b_k(L) = \frac{b_{0k}}{\cos L}, \qquad \text{and} \qquad c_k(L) = c_{0k}. \quad (10)$$

Figures 1(a)–1(d) display correlations with the center location on 45°N for various values of $a_{0k}$, $b_{0k}$, and $c_{0k}$. The value of $c_{01}$ controls the flow across longitudes, which can be seen by comparing two different values, $-7.05$ and $-.353$ [Figures 1(a) and 1(b)]. The speed of flow is greatly reduced, so that $c_{01} = -.353$ gives a process that is nearly fully symmetric. More generally,



Reproduced with permission of the copyright owner. Further reproduction prohibited without permission.

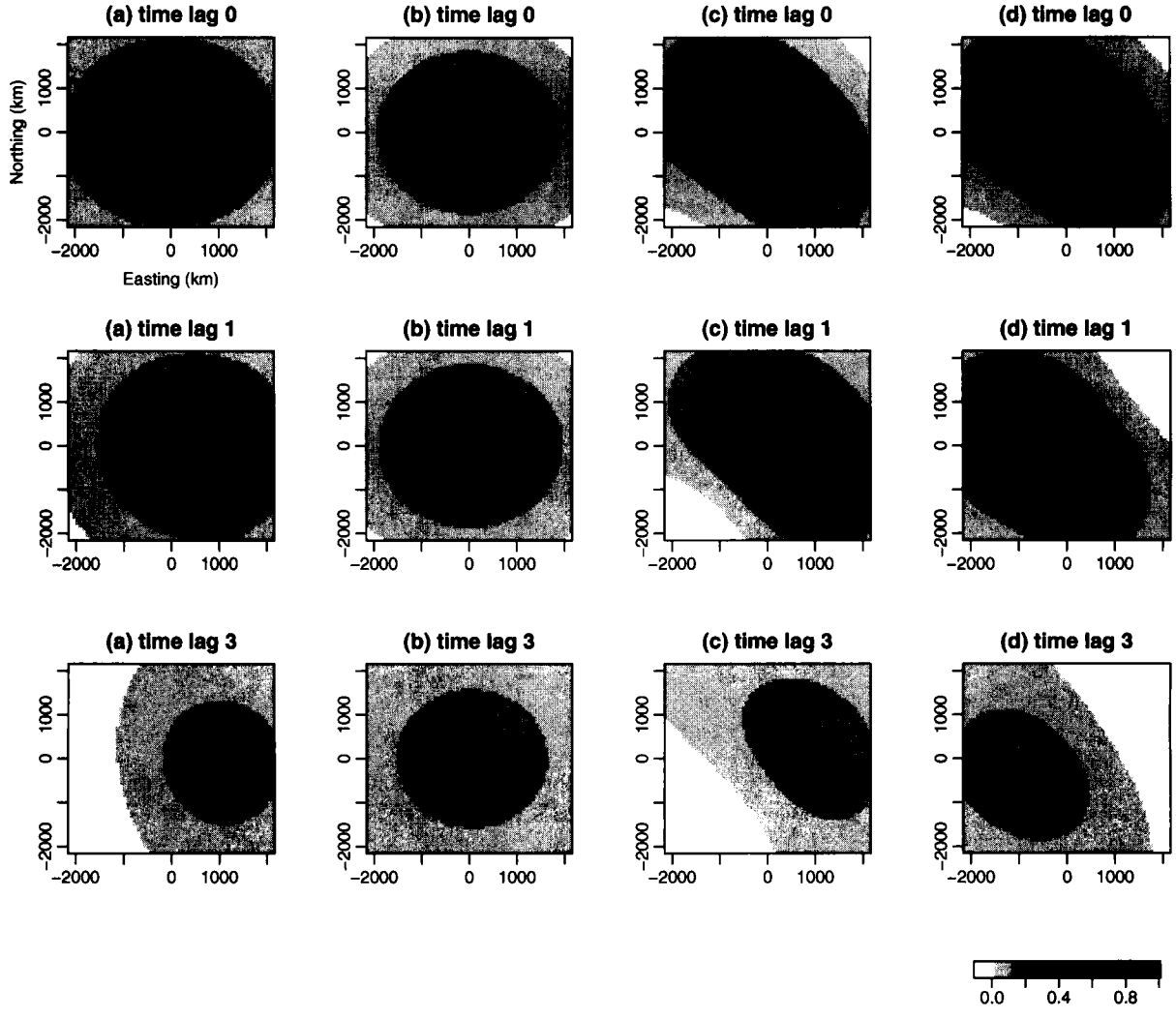


Figure 1. Contour plots of correlations, $K_Y(45°, L, l, -t)/\sqrt{K_Y(45°, 45°, 0, 0)K_Y(L, L, 0, 0)}$, at time lag $t = 0, 1, 3$. For (a), the parameter values come from the estimates of the reduced model in Table 1. The parameter values for (b) are the same as those for (a), except that $c_{01}$ is $-.353$. For (c), the parameter values come from the estimates of the full model in Table 1. The parameter values for (d) are the same as for (c), except that $c_{01}$ and $c_{02}$ change signs. Note that (a) and (b) are from reduced models and (c) and (d) are from full models.

the ratios $|c_{0k}/a_{0k}|$ and $|c_{0k}/b_{0k}|$ control the speed of the movement of the contours with time.

If asymmetries are largely dependent on just longitude and time (Gneiting 2002; Jun and Stein 2004; Stein 2005a), then we may want to avoid the interaction between latitude and longitude or latitude and time. We call $K_Y$ a *reduced model* if we allow only the interaction between longitude and time ($a_{01}$, $b_{02}$, and $c_{02}$ set to 0) and call it a *full model* otherwise. Figures 1(c) and 1(d) show full models, and Figures 1(a) and 1(b) show reduced models. For the full model in Figure 1(c), as time lag increases, the contours shift slightly northward, but there is no shift for the reduced model in Figures 1(a) and 1(b).

Now we compare the condition in (10) with $c_k(L) = c_{0k} \cos L$, keeping $a_k$ and $b_k$ as in (10). The center location is at 35°N in Figures 2(a) and 2(c) and at 65°N in Figures 2(b) and 2(d). Whereas (10) gives a similar speed of flow at both center locations [note the similarity between (a) and (b)], the speed is much slower at 65°N when $c_k(L) = c_{0k} \cos L$ [note how the contours do not move as much in (d) as in (c)]. Therefore, $c_k(L) = c_{0k} \cos L$ [Figs. 2(c) and 2(d)] is similar to rotation models in the sense that the speed of flow slows as we move toward the poles.

## 5. CHARACTERISTICS OF THE NEW COVARIANCE FUNCTION

This section considers the characteristics of our new covariance functions in more detail. One important aspect of our approach is that starting with $K$ having simple space–time structure such as full symmetry, we get $K_Y$, which can have a rich variety of space–time asymmetries on $\mathcal{S}_r^2 \times \mathbb{R}$. Note that (5) and (6) allow $K_Y$ to be space–time asymmetric. In fact, we have

$$\begin{aligned} &K_Y(L_1, L_2, l, t) - K_Y(L_1, L_2, l, -t) \\ &= 2\sum_{k=1}^{N}\big[-a_k(L_1)c_k(L_2)K^{(1,0,0,1)}(L_1, L_2, l, t) \\ &\qquad + a_k(L_2)c_k(L_1)K^{(0,1,0,1)}(L_1, L_2, l, t) \\ &\qquad - \{b_k(L_1)c_k(L_2) + b_k(L_2)c_k(L_1)\} \\ &\qquad \times K^{(0,0,1,1)}(L_1, L_2, l, t)\big], \end{aligned}$$



Reproduced with permission of the copyright owner. Further reproduction prohibited without permission.

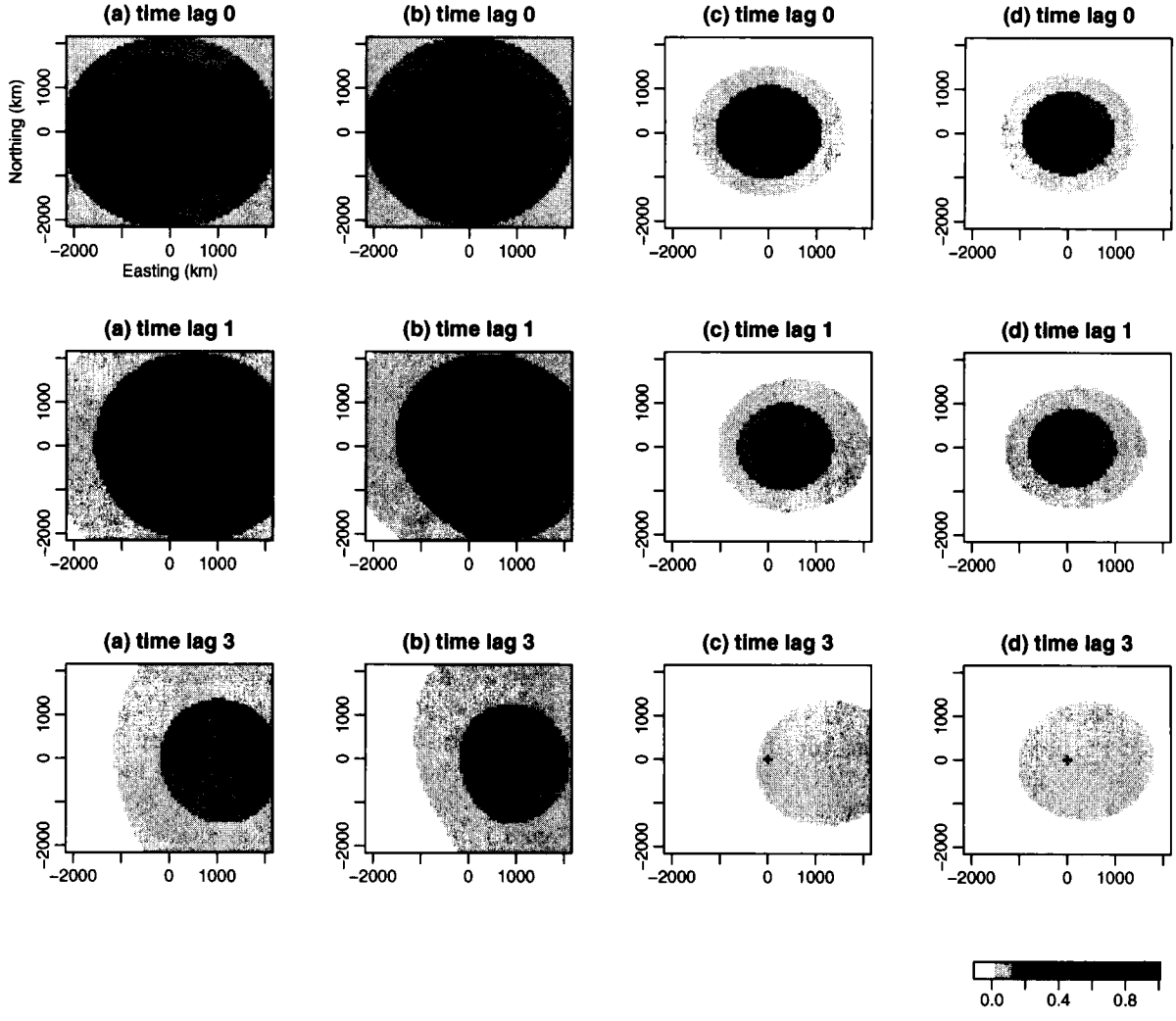


Figure 2. (a) Correlation $K_Y(35°, L, l, -t)/\sqrt{K_Y(35°, 35°, 0, 0)K_Y(L, L, 0, 0)}$ with the condition (10). (b) Correlation $K_Y(65°, L, l, -t)/\sqrt{K_Y(65°, 65°, 0, 0)K_Y(L, L, 0, 0)}$ with the condition (10). (c) The same as (a), except that $c_k(L) = c_{0k}\cos L$. (d) The same as (b), except that $c_k(L) = c_{0k}\cos L$. For (a)–(d), $t = 0, 1, 3$, and the parameter values are the same as the estimates from the reduced model in Table 1.

which depends on $a_k$, $b_k$, and $c_k$ through $a_k c_k$ and $b_k c_k$. For example, Figures 1(b) and 1(d) show that simply changing the signs of $c_{01}$ and $c_{02}$ results in very different shapes of asymmetries. The following result shows how the temporal covariance function at a given site depends on latitude.

*Theorem.* For $t \neq 0$,

$$K_Y(L, L, 0, t) = d_0^2 f(\beta_2|t|) - \sum_{k=1}^{N}\left[\left\{f''(\beta_2|t|) - \frac{f'(\beta_2|t|)}{\beta_2|t|}\right\}\beta_2^2 c_k^2(L) + \frac{f'(\beta_2|t|)}{\beta_2|t|}\{\beta_1^2 r^2 a_k^2(L) + \beta_1^2 r^2 b_k^2(L)\cos^2 L + \beta_2^2 c_k^2(L)\}\right]$$

and

$$K_Y(L, L, 0, 0) = d_0^2 f(0) - f''(0)\sum_{k=1}^{N}\{\beta_1^2 r^2 a_k^2(L) + \beta_1^2 r^2 b_k^2(L)\cos^2 L + \beta_2^2 c_k^2(L)\}. \quad (11)$$

The proof of this theorem is given in Appendix B. This result demonstrates that if $a_k^2(L) + b_k^2(L)\cos^2 L$ and $c_k^2(L)$ are constant for every $k = 1, \ldots, N$, then the purely temporal covariance function of $Y$ does not depend on latitude.

The condition (10) is an example for which $a_k^2(L) + b_k^2(L) \times \cos^2 L$ and $c_k^2(L)$ are constants for every $k = 1, \ldots, N$. Another possibility is

$$a_k(L) = a_{0k}\sin L, \qquad b_k(L) = a_{0k}, \qquad \text{and} \qquad c_k(L) = c_{0k}. \quad (12)$$

The form (12) is somewhat limited in that the same coefficient $a_{0k}$ appears in both $a_k$ and $b_k$. Thus, with (12), if we introduce an interaction between longitude and time, then we automatically introduce an interaction between latitude and time as well. With (10), the covariance function $K_Y$ has another nice simplification: $K_Y(L_1, L_2, 0, t)$ depends on $L_1$ and $L_2$ only through $L_1 - L_2$, although this is not true when the longitude lag is not 0. This simplification does not hold under (12). The forms in (10) and (12) are for the situation where we want $K_Y(L, L, 0, t)$ independent of $L$ for $t \in \mathbb{R}$; however, how to choose the forms of these $a$, $b$, and $c$ functions in general is a problem to be pursued.



Reproduced with permission of the copyright owner. Further reproduction prohibited without permission.

Although $Y(L, l, t)$ is obviously mean square continuous when $Y$ is away from the poles (assuming that $Y$ has continuous mean), it may not be at the poles. Longitude is not defined at the poles, and for any two points near the poles, the chordal distance between the two points is small, but their longitude lag can take any value in $\mathbb{T}$. Suppose that a sequence $\{L_n : L_n \in [0, \frac{\pi}{2}],\ n \in \mathbb{N}\}$ converges to $\frac{\pi}{2}$ as $n \to \infty$. Then we can show that for any $N \in \mathbb{N}$, there exists $\delta > 0$ such that for every $n, m > N$, $E\{Y(L_n, l_1, t) - Y(L_m, l_2, t)\}^2 > \delta$ for $l_1, l_2 \in \mathbb{T}$, $l_1 \neq l_2$, and $t \in \mathbb{R}$. This result follows from

$$\lim_{L_1, L_2 \to \pi/2} K_Y(L_1, L_2, l, 0) = -f''(0)\beta_1^2 R^2 \sum_{k=1}^{N} \widetilde{q}_k \cos l + d_0^2 K(0),$$

where $\widetilde{q}_k = \lim_{L \to \pi/2}\{a_k^2(L) + b_k^2(L)\cos^2 L\} \geq 0$. Because $f \in \mathcal{K}$, $f''(0) \neq 0$ unless $f$ is constant. Therefore, $Y(L, l, t)$ is mean square continuous at the poles only if $\widetilde{q}_k = 0$ for every $k = 1, \ldots, N$.

## 6. APPLICATION TO GLOBAL TOTAL COLUMN OZONE LEVELS

### 6.1 Data

We consider total column ozone data from the World Ozone and Ultraviolet Radiation Data Centre (WOUDC) (*http://www.woudc.org*). We use daily averages of total column ozone levels (measured in Dobson units DUs) from 1957 to 2005 at stations located at 30°N latitude or higher. We choose this range of latitudes for two reasons: to minimize the gaps between the observation sites caused by the lack of sites over the oceans, and because over this domain, we should see clear space–time asymmetry due to the transport by the jet stream. We consider only January 1–15 to avoid seasonality in the covariance structure. There were a total of 160 stations over our domain during this time period. We drop some locations where we have very few observations, leaving 116 stations (Fig. 3). Because many stations were in operation for only a short time, only about 31% of the potential $15 \times 116 \times 49$ observations are available, giving a total of 55,102 observations.

### 6.2 Space–Time Models

Our domain covers the whole range of longitudes, so that the sphericity of the Earth's surface cannot be avoided. Fang and Stein (1998) showed a clear space–time asymmetry of total column ozone levels along the E–W direction over our domain. We model the logarithm of the observed ozone values as a Gaussian random field. Write $O(L, l, t)$ for the observed log total column ozone levels at latitude $L$, longitude $l$, and time $t$.

In modeling a space–time process, it is natural to decompose the random field $O$ as

$$O(L, l, t) = m(L, l) + n(t) + e(L, l, t), \tag{13}$$

that is, a purely spatial term $m$, a purely temporal term $n$, and the residual field $e$. The $n$ term assigns unknown constant means for each of $15 \times 49$ days in the study period. Because we are using only 15 days of data each year, there should not be a strong seasonal pattern in the covariance structure. Throughout the article, spatial average means a spatial surface of averages over time (both years and days) of observed log ozone levels ($O$). Temporal average means a time series of averages over space and years (but not days) of log ozone levels. Figure 4(a) shows that temporal averages have a clear pattern, and thus we assign an unknown constant mean for each of the 15 days. Spatial averages show that ozone levels are consistently high or low at some places (see Fig. 3), and the $m$ term in (13) is necessary to capture these patterns. We model $m$ as a Gaussian random field with mean 0 and a variogram model, $\frac{1}{2}\operatorname{var}[m(L_1, l_1) - m(L_2, l_2)] = \eta\, \mathrm{ch}(L_1, L_2, l_1 - l_2)$ with $\eta > 0$. Figure 4(b) shows that spatial averages have fairly large variation. The residual field, $e$, is modeled as a Gaussian random field, independent of $m$, and is assumed to be independent from year to year. Note that $O$ is not independent across years, due to the presence of the $m$ term. The $e$ field has mean 0 and covariance function

$$\begin{aligned} &\operatorname{cov}\big(e(L_1, l_1, t_1), e(L_2, l_2, t_2)\big) \\ &\quad = K_Y(L_1, L_2, l_1 - l_2, t_1 - t_2) \qquad (14) \\ &\qquad + \delta_1 \exp\left(-\frac{|t_1 - t_2|}{\delta_2}\right) \mathbf{1}_{(L_1 - L_2 = l_1 - l_2 = 0)} \qquad (15) \end{aligned}$$

with $\delta_1$, $\delta_2 > 0$. The function $K_Y$ in (14) is the Matérn-like model given in (9) [a special case of (7) with $N = 2$] and the condition (10). This term will capture the space–time asymmetry in the data. The term in (15) is a spatial nugget term (Gneiting 2002). We first tried fitting models without this term and

Figure 3. The 116 station locations. Symbols indicate the quartile for the average at that station among the 116 station averages (○ 75–100%; △ 50–75%; + 25–50%; × 0–25%).



Reproduced with permission of the copyright owner. Further reproduction prohibited without permission.

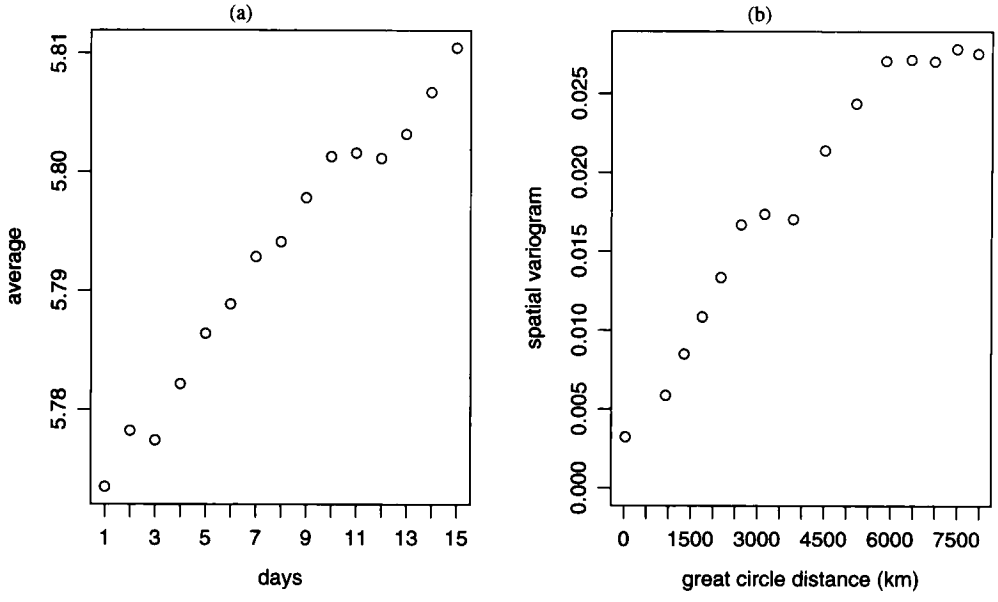


Figure 4. (a) Temporal averages for each day; (b) spatial variogram of spatial averages.

found that the fit was not good. This may be due to the constraint of the model (9) that the process has the same smoothness in space and time. We also tried several other covariance functions for this spatial nugget term. When we used a Matérn covariance function, some parameters were poorly estimated. We reduced the number of parameters by using the exponential covariance function instead of the Matérn covariance function. We originally included an overall nugget term in the covariance function for the $e$ term, but the fitted result was not any better than the result without this term.

In estimating $K_Y$ in (14), if all of the $a_{0k}$, $b_{0k}$, and $c_{0k}$'s are allowed to vary freely, an identifiability problem arises. First, for the full model, permuting the values of $k$ in $\{a_{0k}, b_{0k}, c_{0k}\}$, $k = 1, \ldots, N$ gives the same model. Second, we cannot distinguish the model (full or reduced) with another model with $a_{0k}$, $b_{0k}$, $c_{0k}$, and $d_0$ multiplied by $\phi > 0$ and $\alpha$ divided by $\phi^{1/2}$. Third, for each $k = 1, \ldots, N$, because $K_Y$ depends on $\{a_{0k}, b_{0k}$, and $c_{0k}\}$ through their squared terms or products of two elements among the three, changing signs of all the three terms gives the same model. Therefore, we set $b_{01} = 1$ and $a_{02} > 0$. We consider two forms for $K_Y$, full and reduced, as described in Section 4. The full model has the range $\mathbb{R}$ for each of $a_{01}$, $b_{02}$, $c_{01}$, and $c_{02}$ and $\mathbb{R}^+$ for $a_{02}$. The reduced model sets $a_{01} = b_{02} = c_{02} = 0$. We also compare the full and reduced models with the model without an asymmetry term, which we call the symmetric model. For the symmetric model, the term in (14) is replaced by a fully symmetric Matérn covariance function, $\alpha \mathcal{M}_\nu(\sqrt{h})$, with $\nu > 0$, and $h$ is as defined in Section 2.

### 6.3 Fitted Results

If there were no missing data, then the covariance matrix of $O$ would be block Toeplitz, which would reduce the computational burden. However, due to irregular missing patterns, dealing with the covariance matrices of $O$ is computationally demanding. Therefore, we estimate the parameters in two steps. Suppose that $O(L, l, t)$ is observed and $O(L, l, s)$ is observed for some $s < t$ (but in the same year). Then define $\Delta O(L, l, t) = O(L, l, t) - O(L, l, t - j)$, where $j$ is the smallest positive integer for which $O(L, l, t - j)$ is observed. Note that $\Delta O$ is free of the $m$ term, and thus the likelihood of $\Delta O$ does not contain the parameter $\eta$. This differencing allows us to estimate the parameters for the space–time interaction without influence from the $m$ term. Because we have separate means for each day, we use the restricted maximum likelihood (REML) method (Corbeil and Searle 1976). From now on, log-likelihood values for $\Delta O$ mean the restricted log-likelihood values. To estimate $\eta$, we assume that the spatial averages have variogram $\eta\,\mathrm{ch}(L_1, L_2, l_1 - l_2)$. Because we have modeled the variogram only for $m$, we fit contrasts of the spatial averages to estimate $\eta$. The spatial averages of $O$ will include at least some variation due to the $e$ term, so $\hat{\eta}$ is likely to have some positive bias.

For computation, we use the *nlm* function in R (*http://www.r-project.org/*) to maximize the likelihoods. The parameter estimates for the full, reduced, and symmetric models and the differences of maximized likelihood values among the three models are given in Table 1. For both the reduced and full models, the likelihood with respect to $d_0$ is very flat, and having $d_0$ does not help improve the fit at all. Therefore, we dropped $d_0$ from both the reduced and full models. The estimated value for $\eta$ from the spatial averages of $O$ is 3.33e−6.

AS shown in Table 1, the reduced model has two more parameters than the symmetric model, and the full model has three more parameters than the reduced model. However, the increase in maximum log-likelihood values from the symmetric model to the reduced model is much higher than that from the reduced model to the full model. This implies that even though the full model fits better than the reduced model, the reduced model explains most of the space–time asymmetry in our data captured by the full model. The parameter estimates for the reduced model are nearly identical to the corresponding parameter estimates for the full model. In performing the numerical optimizations, we tried several different initial values for both the reduced and full models (and symmetric models).



Reproduced with permission of the copyright owner. Further reproduction prohibited without permission.

Table 1. Parameter estimates from the symmetric, reduced, and full models from REML and the differences of maximum log-likelihood values of the models to the maximum log-likelihood value of the symmetric model

| | | Symmetric | Reduced | Full |
|---|---|---|---|---|
| 1/(spatial range) ($10^3$ km$^{-1}$) | $\widehat{\beta}_1$ | 1.08 | .76 | .73 |
| 1/(temporal range) (day$^{-1}$) | $\widehat{\beta}_2$ | .79 | .60 | .59 |
| smoothness | $\widehat{\nu}$ | .76 | .74 | .71 |
| | $\widehat{\alpha}$ | 8.69e−3 | 1.86e−4 | 2.02e−4 |
| Asymmetry parameter | $\widehat{a}_{01}$ | | | −.57 |
| Asymmetry parameter | $\widehat{c}_{01}$ | | −7.05 | −6.53 |
| Asymmetry parameter | $\widehat{a}_{02}$ | | 1.05 | .85 |
| Asymmetry parameter | $\widehat{b}_{02}$ | | | .052 |
| Asymmetry parameter | $\widehat{c}_{02}$ | | | −.12 |
| Sill for spatial nugget | $\widehat{\delta}_1$ | 8.64e−4 | 8.48e−4 | 7.74e−4 |
| Range of spatial nugget (day) | $\widehat{\delta}_2$ | .35 | .32 | .41 |
| Differences in log-likelihood | $\Delta$llik | 0 | 471.76 | 595.14 |

NOTE: The maximum (restricted) log-likelihood value of the symmetric model is 48,599.36. For identifiability, we set $b_{01} = 1$ and $a_{02} > 0$.

Thus these similar values are not an artifact of how starting values were selected. The estimates for $b_{0k}$ and the $c_{0k}$ for both models show similar patterns in the sense that the $\widehat{c}_{0k}$'s have large magnitude and the signs of the $\widehat{c}_{0k}$'s are different from the signs of the $\widehat{b}_{0k}$'s. Except for $\alpha$, the parameter estimates for the symmetric model are very similar to those for the asymmetric (full and reduced) models. Interpretation of $\alpha$ is different for the asymmetric and symmetric models, so these estimates are not comparable. The consistent values of the other parameter estimates for the three different models (symmetric, reduced and full) may be a sign that our parameter estimates measure stable and interpretable properties of the process.

Now we compare the empirical and fitted covariances from the three models. Figure 5 shows the empirical spatial and temporal variograms and corresponding fitted values from the three models. The spatial variogram for $O$ would include the effect of the $m$ term, so we instead present the spatial variogram for $\Delta_1 O$ ($\Delta_1 O(L, l, t) = O(L, l, t) - O(L, l, t-1)$) rather than for $O$. Note that $\Delta_1 O$ is available only when both $O(L, l, t)$ and $O(L, l, t-1)$ are observed. We bin the averaged spatial variograms and display averages and quantiles in Figure 5. Bins are determined so that an almost equal number of values belongs to each bin. For the temporal variogram, we first calculate the temporal variogram at each spatial location and then average those across locations. Because the temporal variogram is free of the $m$ term, we display the temporal variogram of $O$. No binning is necessary in this case. Fitted values from both the full and reduced models match the empirical spatial and temporal variograms quite well. Fitted values of the purely temporal covariance $K_Y(L, L, 0, t)$ from both the full and reduced models are identical for different latitudes $L$ (not shown). As explained in Section 5, this is because of the condition (10) for the functions $a$, $b$, and $c$.

One of the main focuses of our approach is to produce space–time asymmetries. We assess how well our new covariance functions explain the asymmetries present in the data. Moreover, we compare our models (both full and reduced models) with the symmetric model to see how much the asymmetry factors in the models improve the fit. For this purpose, we define the empirical space–time variogram

$$V(\mathbf{s}_i, \mathbf{s}_j; k) = \frac{1}{2N_{ijk}} \sum_{t \in T_{ijk}} \{O(\mathbf{s}_i, t+k) - O(\mathbf{s}_j, t)\}^2$$

for $k \in \mathbb{Z}$. Here $T_{ijk}$ denotes the set of time points, $t$, for which $O(\mathbf{s}_i, t+k)$ and $O(\mathbf{s}_j, t)$ are both observed and $N_{ijk}$ denotes the number of time points in $T_{ijk}$. Then $\Delta_{ijk} = V(\mathbf{s}_i, \mathbf{s}_j; k) - V(\mathbf{s}_i, \mathbf{s}_j; -k)$ should represent the magnitude of the asymmetry. For example, when $\mathbf{s}_i$ is east of $\mathbf{s}_j$ and $k$ is positive, $\Delta_{ijk} < 0$ means that there is asymmetry due to flow from west to east, $\Delta_{ijk} = 0$ means that there is no asymmetry, and $\Delta_{ijk} > 0$ means

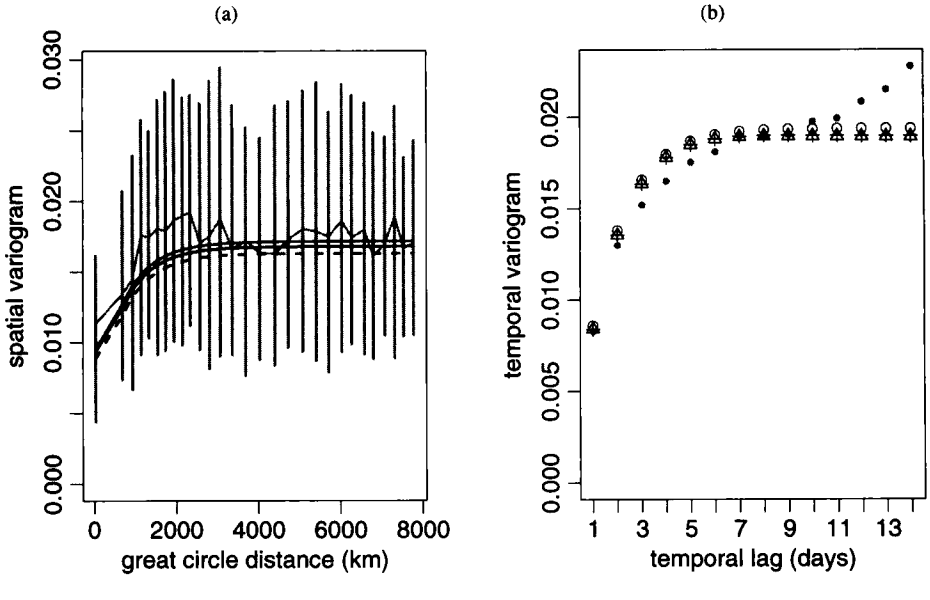


Figure 5. Comparison of spatial (a) and temporal (b) variograms for the observations and the fitted values from the full and reduced models. For the spatial variogram, quantiles (10%, 90%) are displayed in bars, and averages are shown in lines. [(a) ——, empirical; ——, symmetric; ——, reduced; – –, full; (b) •, empirical; ○, symmetric; △, reduced; +, full.]



Reproduced with permission of the copyright owner. Further reproduction prohibited without permission.

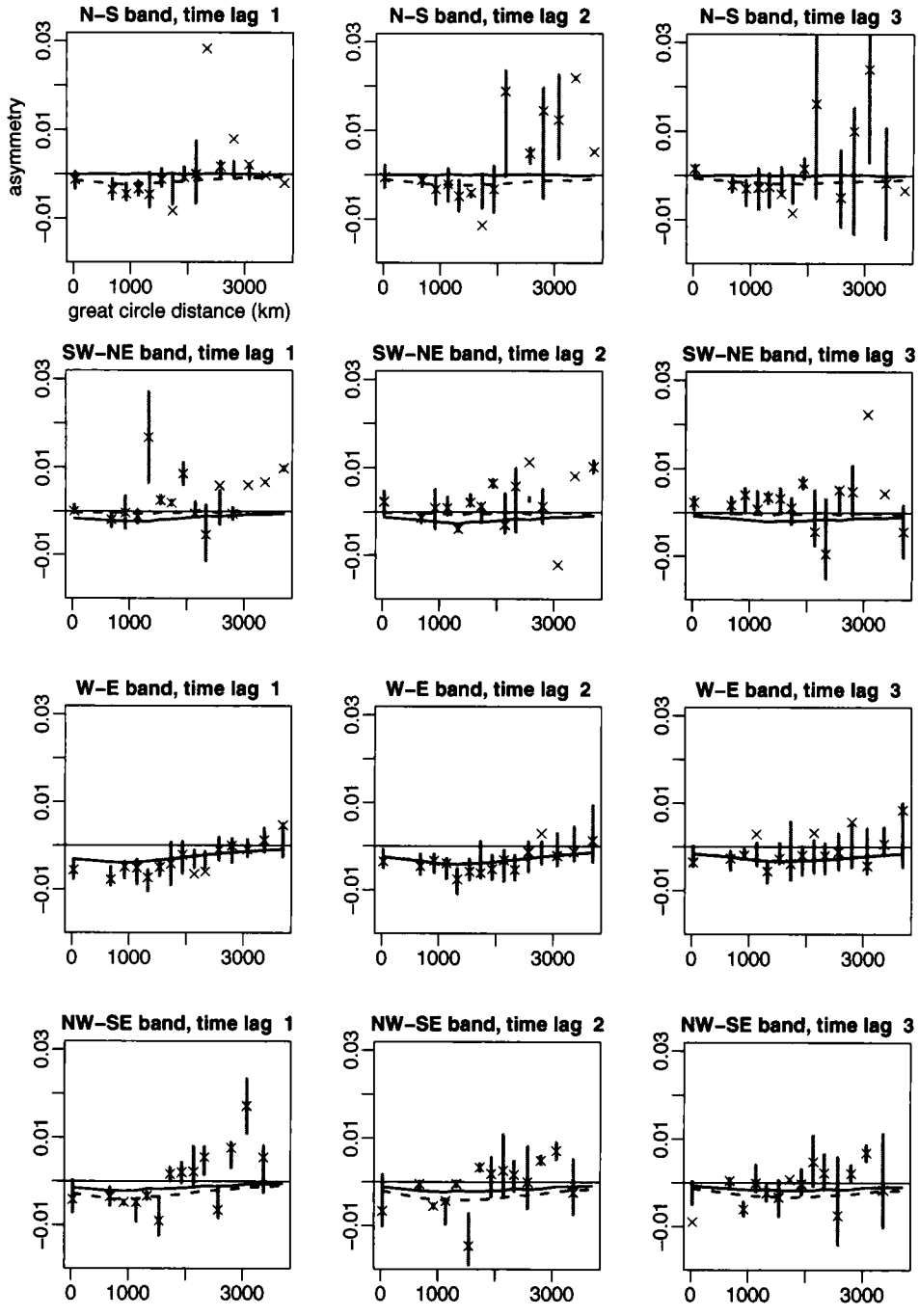


Figure 6. Comparison of $\Delta_{ijk}$ ($k = 1, 2, 3$) for the data and the fitted values from the full and reduced models. (—×— empirical; —— reduced; – – full.) For the empirical values, the average and the 25th and 75th percentiles are displayed. For the fitted values, only averages are displayed

that there is asymmetry due to flow from east to west. It is worth pointing out that $E\Delta_{ijk}$ is not affected by the $m$ term, although the variance of $\Delta_{ijk}$ is.

Figure 6 shows the empirical and fitted values (from the full and reduced models) of $\Delta_{ijk}$ for $k = 1, 2, 3$. The symmetric model gives 0 as the estimated value of $\Delta_{ijk}$. The sites $\mathbf{s}_i$ and $\mathbf{s}_j$ are chosen from the 116 sites in such a way that $\mathbf{s}_i$ is always south of $\mathbf{s}_j$ (N–S band), northeast of $\mathbf{s}_j$ (SW–NE band), east of $\mathbf{s}_j$ (W–E band) and southeast of $\mathbf{s}_j$ (NW–SE band). Bins are chosen so that an almost equal number of values belongs to each. In comparing the empirical to the fitted values, overall, the empirical values match the fitted values fairly well for both the full and reduced models. The data suggest that the asymmetries due to westerly and northwesterly flow are stronger than those for the other two directions. This is not surprising, because there is a predominantly westerly flow over the northern hemisphere, especially at latitude 30°N or higher. The fitted values from both the full and reduced models match this pattern in the data fairly well, and the full model does better at asymmetries for N–S and NW–SE bands than the reduced model. Because there is no interaction between latitude and time in the reduced model, the fitted values from the reduced model do not show any asymmetry in the N–S direction, whereas those from the full model do. On the other hand, the two models give almost the same



Reproduced with permission of the copyright owner. Further reproduction prohibited without permission.

amount of asymmetry in the W–E direction. For this direction, the locations of maximum asymmetry from both models move toward longer distance lags with increasing time lag, which apparently represents the transport of ozone with the dominant stratospheric winds.

We also examine the fitted values of $K_Y$ for both the full and reduced models using contour plots. Figures 1(a) and 1(c) plot the fitted $K_Y$ in correlation scale. Figure 1(a) shows the fitted $K_Y$ value (in correlation scale) for the reduced model, and Figure 1(c) shows this value for the full model. As time lag increases, both fits show movement of the flow from west to east. At each time lag, correlations are strongest in the NW–SE direction for the full model, whereas the reduced model gives nearly isotropic correlation structure. Comparing the contours with different center locations along latitudes shows that unlike the rotation models, $K_Y$ implies that the speed of the flow is not different at different latitudes [Figs. 2(a) and 2(b)].

## 7. REMARKS

In our analysis, we used the condition (10), so that the covariance model implies constant transport rates at different latitude levels. This condition may be fairly realistic in this analysis, because our latitude range is only 30°N and higher. However, it is known that wind speed is slowest in the tropics (0°N–30°N), strongest in the mid-latitudes (30°N–60°N), and intermediate in the upper latitudes (60°N–90°N) (Peixóto and Oort 1984). Therefore, if we were to look at a wider range of latitudes, then we should let the functions $a$, $b$, and $c$ vary along the latitudes in such a way that the covariance function can reflect these wind patterns. Certainly, the rotation models are not capable of capturing these patterns.

We estimated the covariance parameters in two steps due to the computational difficulty caused by the $m$ term. Because we have a common $m$ term every year, the covariance matrix for $O$ is not a block diagonal matrix. Note that the dimension of the covariance matrix for $O$ is $55{,}102 \times 55{,}102$. Moreover, due to different missing patterns every year, the covariance matrix for $O$ comprises blocks of different sizes, making computation more difficult. However, the fact that $m$ has the same covariance function for each year and $e$ is independent over years provide opportunities for more efficient matrix computations. We have begun investigating ways of exactly calculating the likelihood for these data and hope to report on them in future work.

By working with contrasts of $O$, we do not need to model either seasonal or long-term effects. It is, of course, interesting to estimate long-term trends in ozone, but one should use all of the data and not just 15 days each year if that is the goal. Here our focus is on the covariance structure on a daily time scale.

One might wonder whether there are any potential outliers/influential points due to remote spatial locations, such as the single location far north in Canada or the single location on Iceland. To check this, we redid the analysis on North America and Northern Eurasia separately. The parameter estimates for the new analysis are very similar to the parameter estimates that we report in Table 1. For example, for the reduced model, the parameter estimates for Northern Eurasia are .78, .60, .71, 1.50e−4, −7.30, 1.09, 8.05e−4, and .34 (following the order of parameters in Table 1). Based on this result, we do not believe that potential outliers/influential points due to remote spatial locations is much of an issue.

## ACKNOWLEDGEMENTS

Most of this work was done as a part of Mikyoung Jun's Ph.D. thesis at the University of Chicago. Although the research described herein has been funded wholly or in part by the United States Environmental Protection Agency (EPA) through STAR Cooperative Agreement R-82940201-0 to the University of Chicago, it has not been subjected to the EPA's required peer and policy review and thus does not necessarily reflect the views of the agency, and no official endorsement should be inferred. Mikyoung Jun also acknowledges the support from the Geophysical Statistics Project, National Center for Atmospheric Research, through U.S. National Science Foundation grant DMS-03-55474. The authors thank the associate editor and two reviewers for their comments, which helped to greatly improve the presentation of the article.

## APPENDIX A: EXPRESSIONS

Here we give explicit expressions for the $h_i$ and $h_{ij}$'s evaluated at latitudes $L_1$ and $L_2$, latitude lag $L = L_1 - L_2$, longitude lag $l = l_1 - l_2$ and time lag $t = t_1 - t_2$:

$$\begin{aligned}
h_1(L_1, L_2, l) &= h_2(L_2, L_1, l) \\
&= 4\beta_1^2 r^2 \left\{ \sin\left(\frac{L}{2}\right)\cos\left(\frac{L}{2}\right) \right. \\
&\qquad \left. - \sin L_1 \cos L_2 \sin^2\left(\frac{l}{2}\right) \right\}; \\
h_3 &= 4\beta_1^2 r^2 \cos L_1 \cos L_2 \sin\left(\frac{l}{2}\right)\cos\left(\frac{l}{2}\right); \\
h_{33} &= 2\beta_1^2 r^2 \cos L_1 \cos L_2 \cos^2\left(\frac{l}{2}\right) \\
&\qquad - 2\beta_1^2 r^2 \cos L_1 \cos L_2 \sin^2\left(\frac{l}{2}\right); \\
h_{12} &= 4\beta_1^2 r^2 \left\{ -\frac{1}{2}\cos^2\left(\frac{L}{2}\right) + \frac{1}{2}\sin^2\left(\frac{L}{2}\right) \right. \\
&\qquad \left. + \sin L_1 \sin L_2 \sin^2\left(\frac{l}{2}\right) \right\}; \\
h_{13}(L_1, L_2, l) &= h_{23}(L_2, L_1, l) \\
&= -4\beta_1^2 r^2 \sin L_1 \cos L_2 \sin\left(\frac{l}{2}\right)\cos\left(\frac{l}{2}\right),
\end{aligned}$$

and

$$h_4 = 2\beta_2^2 t, \qquad h_{44} = 2\beta_2^2, \qquad h_{14} = h_{24} = h_{34} = 0.$$

Explicit expressions for $C_1$ and $C_2$ in (9) are given by

$$\begin{aligned}
C_1 = \frac{\alpha}{4} \sum_{k=1}^{N} \{ & a_k(L_1)a_k(L_2)h_1h_2 - b_k(L_1)b_k(L_2)h_3^2 \\
& - c_k(L_1)c_k(L_2)h_4^2 - a_k(L_1)b_k(L_2)h_1h_3 \\
& + a_k(L_2)b_k(L_1)h_2h_3 - a_k(L_1)c_k(L_2)h_1h_4 \\
& + a_k(L_2)c_k(L_1)h_2h_4 - b_k(L_1)c_k(L_2)h_3h_4 \\
& - b_k(L_2)c_k(L_1)h_3h_4 \} + \alpha h d_0^2
\end{aligned}$$



Reproduced with permission of the copyright owner. Further reproduction prohibited without permission.

and

$$C_2 = -\frac{\alpha}{2}\sum_{k=1}^{N}\{a_k(L_1)a_k(L_2)h_{12} - b_k(L_1)b_k(L_2)h_{33} - c_k(L_1)c_k(L_2)h_{44} - a_k(L_1)b_k(L_2)h_{13} + a_k(L_2)b_k(L_1)h_{23}\} + 2\alpha\nu d_0^2.$$

## APPENDIX B: PROOF OF THE THEOREM

For $t \in \mathbb{R}$ and $t \neq 0$,

$$\frac{f'(\sqrt{h})}{\sqrt{h}} = \frac{f'(\beta_2|t|)}{\beta_2|t|} + o(1) \quad \text{and}$$

$$f''(\sqrt{h}) = f''(\beta_2|t|) + o(1) \quad \text{as } l \to 0.$$

Then from (7) and (8), the expressions given in Appendix A, and $h_1, h_2, h_3 \to 0$ as $l \to 0$, the leading term of $K_Y(L, L, l, t)$ as $l \to 0$ is given by

$$-\left\{f''(\beta_2|t|) - \frac{f'(\beta_2|t|)}{\beta_2|t|}\right\}\frac{1}{4h(L,L,0)}\sum_k c_k^2(L)h_4^2(L,L,0) + \frac{f'(2\beta_2|t|)}{\beta_2|t|}\sum_k\left\{a_k^2(L)h_{12}(L,L,0) - b_k^2(L)h_{33}(L,L,0) - c_k^2(L)h_{44}(L,L,0)\right\}. \tag{A.1}$$

When $t = 0$,

$$\frac{f'(\sqrt{h})}{\sqrt{h}} = f''(0) + o(1) \quad \text{and}$$

$$f''(\sqrt{h}) = f''(0) + o(1) \quad \text{as } l \to 0,$$

and (A.1) should be modified accordingly.

*[Received December 2005. Revised November 2006.]*

## REFERENCES


Abramowitz, M., and Stegun, I. A. (eds.) (1965), *Handbook of Mathematical Functions* (9th ed.), New York: Dover.

Corbeil, R., and Searle, S. (1976), "Restricted Maximum Likelihood (REML) Estimation of Variance Components in the Mixed Model," *Technometrics*, 18, 31–38.

Cressie, N. A. (1993), *Statistics for Spatial Data* (rev. ed.), New York: Wiley.

Cressie, N. A., and Huang, H.-C. (1999), "Classes of Nonseparable, Spatiotemporal Stationary Covariance Functions," *Journal of the American Statistical Association*, 94, 1330–1340.

Das, B. (2000), "Global Covariance Modeling: A Deformation Approach to Anisotropy," unpublished doctoral dissertation, University of Washington, Dept. of Statistics.

de Iaco, S., Myers, D., and Posa, D. (2002), "Nonseparable Space–Time Covariance Models: Some Parametric Families," *Mathematical Geology*, 34, 23–42.

Fang, D., and Stein, M. L. (1998), "Some Statistical Methods for Analyzing the TOMS Data," *Journal of Geophysical Research*, 103 (D20), 26165–26182.

Gaspari, G., and Cohn, S. E. (1999), "Construction of Correlation Functions in Two and Three Dimensions," *Quarterly Journal of the Royal Meteorological Society*, 125, 723–757.

Gneiting, T. (1999), "Correlation Functions for Atmospheric Data Analysis," *Quarterly Journal of the Royal Meteorological Society*, 125, 2449–2464.

——— (2002), "Nonseparable, Stationary Covariance Functions for Space–Time Data," *Journal of the American Statistical Association*, 97, 590–600.

Grafarend, E. W. (1976), "Geodetic Application of Stochastic Processes," *Physics of the Earth and Planetary Interiors*, 12, 151–179.

Haas, T. C. (1995), "Local Prediction of a Spatio-Temporal Process With an Application to Wet Sulfate Deposition," *Journal of the American Statistical Association*, 90, 1189–1199.

Jones, R. H. (1963), "Stochastic Processes on a Sphere," *The Annals of Mathematical Statistics*, 34, 213–218.

Jones, R. H., and Zhang, Y. (1997), *Modeling Longitudinal and Spatially Correlated Data*, New York: Springer-Verlag, pp. 289–298.

Jun, M., and Stein, M. L. (2004), "Statistical Comparison of Observed and CMAQ Modeled Daily Sulfate Levels," *Atmospheric Environment*, 38, 4427–4436.

Ma, C. (2003), "Families of Spatio-Temporal Stationary Covariance Models," *Journal of Statistical Planning and Inference*, 116, 489–501.

McLeod, M. G. (1986), "Stochastic Processes on a Sphere," *Physics of the Earth and Planetary Interiors*, 43, 283–299.

——— (1996), "Spatial and Temporal Power Spectra of the Geomagnetic Field," *Journal of Geophysical Research*, 101 (B2), 2745–2763.

Mitchell, M. W., and Gumpertz, M. L. (2003), "Spatio-Temporal Prediction Inside a Free-Air $CO_2$ Enrichment System," *Journal of Agricultural, Biological & Environmental Statistics*, 8, 310–327.

Oh, H.-S., and Li, T.-H. (2004), "Estimation of Global Temperature Fields From Scattered Observations by a Spherical-Wavelet-Based Spatially Adaptive Method," *Journal of the Royal Statistical Society*, Ser. B, 66, 221–238.

Peixóto, J. P., and Oort, A. H. (1984), "Physics of Climate," *Reviews of Modern Physics*, 56, 365–429.

Posa, D. (1993), "A Simple Description of Spatial-Temporal Processes," *Computational Statistics and Data Analysis*, 15, 425–437.

Schreiner, M. (1997), "On a New Condition for Strictly Positive Definite Functions on Spheres," in *Proceedings of the American Mathematical Society*, Vol. 125, pp. 531–539.

Stein, M. L. (1999), *Interpolation of Spatial Data: Some Theory for Kriging*, New York: Springer-Verlag.

——— (2005a), "Space–Time Covariance Functions," *Journal of the American Statistical Association*, 100, 310–321.

——— (2005b), "Statistical Methods for Regular Monitoring Data," *Journal of the Royal Statistical Society*, Ser. B, 67, 667–687.

Weber, R. O., and Talkner, P. (1993), "Some Remarks on Spatial Correlation Function Models," *Monthly Weather Review*, 232, 2611–2617.

Yaglom, A. M. (1961), "Second-Order Homogeneous Random Fields," *Proceedings of the Fourth Berkeley Symposium in Mathematical Statistics and Probability Theory*, 2, 593–622.

——— (1987), *Correlation Theory of Stationary and Related Random Functions*, Vol. I, New York: Springer-Verlag.




Reproduced with permission of the copyright owner. Further reproduction prohibited without permission.